The Journal of Experimental Biology 211, 731-740
Published by The Company of Biologists 2008
doi:10.1242/jeb.011148

Physiological characterization of stolon regression in a colonial hydroid

Kimberly S. Cherry Vogt, Gabrielle C. Geddes, Lori S. Bross and Neil W. Blackstone*

Department of Biological Sciences, Northern Illinois University, DeKalb, IL 60115, USA

*Author for correspondence (e-mail: neilb@niu.edu)

Accepted 24 December 2007

SUMMARY

As with many colonial animals, hydractiniid hydroids display a range of morphological variation. Sheet-like forms exhibit feeding polyps close together with short connecting stolons, whereas runner-like forms have more distant polyps and longer connecting stolons. These morphological patterns are thought to derive from rates of stolon growth and polyp formation. Here, stolon regression is identified and characterized as a potential process underlying this variation. Typically, regression can be observed in a few stolons of a normally growing colony. For detailed studies, many stolons of a colony can be induced to regress by pharmacological manipulations of reactive oxygen species (e.g. hydrogen peroxide) or reactive nitrogen species (e.g. nitric oxide). The regression process begins with a cessation of gastrovascular flow to the distal part of the stolon. High levels of endogenous H_2O_2 and NO then accumulate in the regressing stolon. Remarkably, exogenous treatments with either H_2O_2 or an NO donor equivalently trigger endogenous formation of both H_2O_2 and NO. Cell death during regression is suggested by both morphological features, detected by transmission electron microscopy, and DNA fragmentation, detected by TUNEL. Stolon regression may occur when colonies detect environmental signals that favor continued growth in the same location rather than outward growth.

Key words: cell death, clonal organism, cnidarian, evolution and development, evolutionary morphology, hydroid, *Podocoryna*, *Podocoryne*, reactive oxygen species, reactive nitrogen species.

INTRODUCTION

As model systems for experimental studies of the evolution of development, clonal organisms (e.g. many fungi, herbaceous plants, and colonial invertebrates) are particularly useful because growth and development are inseparable, providing a broad chronological window in which manipulation is possible (Blackstone, 1997; van Kleunen and Fisher, 2001). In these clonal groups, the morphology can be idealized as comprising feeding and reproductive units, here termed polyps, which are interconnected by vascular stolons. Runner-like forms show widely spaced polyps and long stolonal connections, whereas sheet-like forms show closely packed polyps with short stolonal connections (Buss and Blackstone, 1991). These different morphological patterns may reflect changes in the timing of the production of polyps and stolon tips relative to rates of stolon growth and colony maturation; high ratios of production yield sheets, and low ratios yield runners.

Colonial hydroids can be particularly useful for investigating the differences between runners and sheets. These hydroids are representatives of cnidarians, a group of early-evolving animals. Considerable research has focused on the mechanisms underlying their development. Early studies concentrated on physiological parameters, particularly gastrovascular flow. For instance, Hale (Hale, 1964) described the growth of stolons in terms of the influence of gastrovascular flow on the cyclic pattern of forward surges and partial backward retraction in the stolon tip. Wyttenbach (Wyttenbach, 1968; Wyttenbach, 1969; Wyttenbach, 1973) further characterized this type of stolon elongation in terms of colony-level variations in growth rate, cycle phases, and features of gastrovascular flow. Beloussov and collaborators (e.g. Beloussov, 1973; Beloussov et al., 1989) also studied stolon tip extension, but from the perspective of cell-level morphogenesis and physiology. Schierwater et al. (Schierwater et al., 1992) provided an overview of the various physiological parameters that contribute to gastrovascular flow and proposed a cellular mechanism for stolonal expansion and contraction. Dudgeon and Buss (Dudgeon and Buss, 1996) also emphasized the importance of gastrovascular flow in colony development. At the same time, a variety of studies focused on the effects of morphogens on colony growth (Plickert et al., 1987) including head activator (Schaller et al., 1989), stolon-inducing factor (Lange and Müller, 1991) and other peptides (Takahashi et al., 1997). More recent studies have begun to elucidate the role of gene activity in colony development. For instance, Cartwright and Buss (Cartwright and Buss, 1999) and Cartwright et al. (Cartwright et al., 1999; Cartwright et al., 2006) explored the expression of a well-studied parahox gene in the various components of the colony whose frequencies and distributions contribute to the overall pattern.

Despite these and other efforts to understand colony development, the relevance of regressive processes has not yet been considered in detail. For instance, stolon regression could influence both runner- and sheet-like patterns: the former could be the result of little regression of peripheral stolons, whereas the latter could be the result of greater amounts of such regression. Increasingly, developmental biologists are recognizing the widespread occurrence and importance of tissue regression and related processes and their contribution to pattern formation. For example, tissue regression plays a role in sculpting the individual digits of the limbs of vertebrates (Zuzarte-Luís and Hurlé, 2002) and the segments of the body of some invertebrates (Lohmann et al., 2002). The regression of the tadpole's tail during its metamorphosis into a frog is another well-known example (Tata, 2006). Tissue regression is also important in the transition of insects from their larval forms to their adult forms and has been described in a variety of species (Hori et al., 2000).

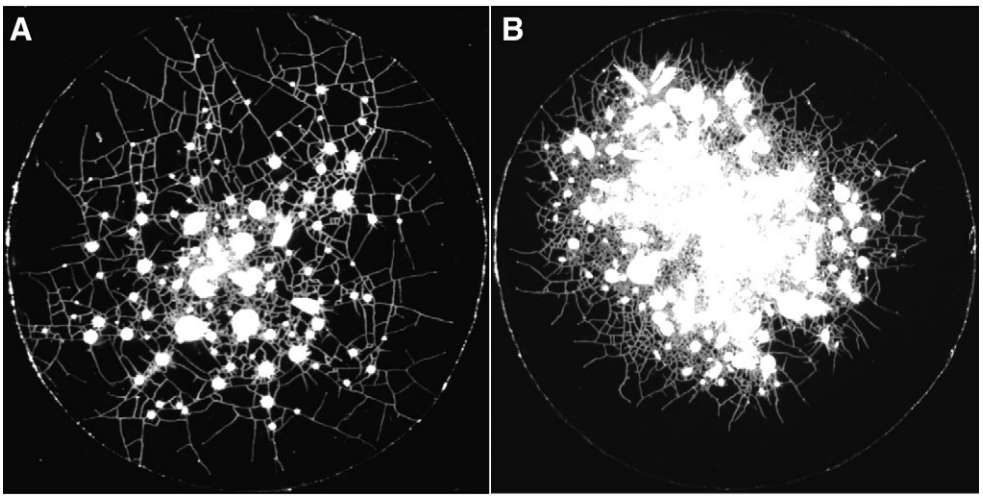

Fig. 1. Images of genetically identical colonies of *P. carnea* growing on 18 mm diameter glass coverslips. Polyps are bright and circular; stolons are darker and web-like. (A) An untreated control colony exhibits a more runner-like morphology. (B) A colony treated with 100 μmol l^{-1} vitamin C exhibits a more sheet-like morphology (see Blackstone et al., 2005).

Tissue regression may be relevant to pattern formation in colonial hydroids. In normally growing colonies, stolons can frequently grow out and then cease to grow or even under some circumstances regress. Stolon regression has been observed in untreated colonies on numerous occasions. While at any given time, only a few stolons in a colony may be regressing, over time such a process could have a cumulative effect on colony morphology. For instance, consider two colonies, one with twice as many regressing stolons at any given time. Over weeks and months of colony development, the resulting difference in morphology could be substantial. Indeed, this change in colony morphology has been detected in colonies treated with vitamin C (Fig. 1). Nevertheless, the number of regressing stolons in colonies treated with vitamin C, though higher than controls, was relatively low and variable. Perhaps surprisingly, however, stolon regression was frequently observed to coincide with high levels of endogenous reactive oxygen species (ROS) production (Blackstone et al., 2004a; Blackstone et al., 2005). Thus, stolon regression may be an active process involving other active processes such as some form of regulated cell death. In this context, we developed a reliable method of pharmacologically inducing stolon regression in a colonial hydroid and have attempted to characterize this process at morphological, physiological and cellular levels.

MATERIALS AND METHODS

Study species and culture conditions

For all investigations, colonies of a single clone of *Podocoryna* (= *Podocoryne*) *carnea* Sars 1846 were cultured using standard methods (e.g. Blackstone, 1999). The clone, designated as P3, has been used in previous studies for over 14 years. All experiments were performed on clonal replicates grown from single polyp explants of a source colony. For each experiment, control and treated colonies were explanted from the same source colony to minimize non-genetic sources of variation (Ponczek and Blackstone, 2001). For measures of ROS, reactive nitrogen species (RNS), gastrovascular flow and cell death, colonies were grown on 15 mm diameter round glass coverslips. For transmission electron microscopy (TEM), clonal replicates were grown on a piece of clear polyethylene tied to a glass slide. All experiments were carried out at 20.5°C.

Treatment with hydrogen peroxide and nitric oxide

For characterization of stolon regression, it was deemed necessary to develop a protocol that reliably triggered the regression of a large number of stolons in a single colony. Since vitamin C-treated colonies typically show a variable response, colonies were treated with hydrogen peroxide (H_2O_2) or a nitric oxide donor, S-nitroso-N-acetyl-penicillamine (SNAP). For all H_2O_2 experiments, colonies were treated in a 5 mmol l^{-1} solution of H_2O_2 and seawater (Vernole et al., 1998) with controls placed in plain seawater. For all NO experiments, colonies were treated in seawater with SNAP dissolved in dimethyl sulfoxide (DMSO) at a final concentration of 0.5 mmol l^{-1}. Controls were treated with an equivalent concentration of DMSO. For both H_2O_2 and NO experiments, a set of 6–7 treated and 6–7 control colonies were incubated for ~60 min beginning 24 h after feeding. Following treatment in respective solutions, the colonies were incubated in plain seawater and staining solution, typically for ~60 min prior to imaging or fixation. Excluding colonies analyzed for several of the cell death assays and for temporal sequence of events, fixation or imaging typically was done 2 h after treatment began.

Measurement of reactive oxygen species

The compound 2′,7′-dichlorodihydrofluorescein diacetate (H_2DCFDA; Molecular Probes, Eugene, OR, USA) was used as a semi-quantitative assay of general oxidative stress (Jantzen et al., 1998). This non-fluorescent dye is taken up by cells, and the acetate groups are removed by intracellular esterases to form H_2DCF. Oxidation within cells leads to the fluorescent product, which can then be visualized using fluorescence microscopy. Molecules that oxidize H_2DCF will typically oxidize cysteine residues, histidine residues and iron-sulfur clusters of proteins. The oxidation of these residues and clusters are among the primary mechanisms by which ROS can affect signaling pathways (Armstrong et al., 2004; Filomeni et al., 2005; Lee and Helmann, 2006; Salmeen et al., 2003; van Montfort et al., 2003). Thus, while there may be some debate as to whether the activation of H_2DCF is specific for the detection of H_2O_2 (Finkel, 2001), this assay quantifies the extent to which potential signaling pathways may be affected. A 10 mmol l^{-1} stock solution of H_2DCFDA was prepared in anhydrous DMSO. After incubation in SNAP or H_2O_2, treatment solutions were replaced with plain seawater and H_2DCFDA was added to each dish to a concentration of 10 μmol l^{-1}. Colonies were then incubated in the dark for ~60 min. Subsequently, each colony was imaged in a microscope chamber containing plain seawater using an Orca-100 camera (Hamamatsu Photonics, Hamamatsu City, Japan) and an Axiovert 135 microscope (Carl Zeiss, Jena, Germany). ROS-related oxidative processes (as indicated by H_2DCFDA-derived

dichlorofluorescein) were imaged for three stolon tips per colony (excitation 450–490 nm, emission 515–565 nm). The luminance and area of each stolon tip was measured in Image-Pro Plus (Media Cybernetics, Silver Spring, MD, USA) by: (1) using a bright-field image of the stolon tip to define the area of the stolon and the area of the background; (2) with these areas serving as 'areas of interest' for the fluorescent image, allowing the software to measure average luminance of both areas; and (3) exporting these measurements to file. The area of each stolon was thus defined, and the luminance of the stolon was adjusted for the background luminance by subtraction. These measures were analyzed by a nested analysis of variance (stolon tips within clonal replicates, clonal replicates within treatments).

Measurement of reactive nitrogen species

The compound 4-amino-5-methylamino-2′,7′-difluorofluorescein (DAF-FM) diacetate (Molecular Probes, Eugene, Oregon, USA) was used as a semi-quantitative indicator of low concentrations of NO (Kojima et al., 1999). This non-fluorescent dye is taken up by cells, and the acetate groups are removed by intracellular esterases to form DAF-FM. Upon reaction with NO, DAF-FM forms a fluorescent benzotriazole derivative. A 2 mmol l^{-1} stock solution of DAF-FM diacetate was prepared in anhydrous DMSO. After incubation of colonies in SNAP or H_2O_2, treatment solutions were replaced with plain seawater, and DAF-FM diacetate stock solution was added to each dish to a concentration of 2 μmol l^{-1}. Colonies were then incubated for ~60 min in the dark prior to measurement. Images were obtained (excitation 450–490 nm, emission 515–565 nm), measured and analyzed as described above.

Cell death analyses

The similar effects of H_2O_2 and SNAP on stolon regression (see Results), as well as clear parallels to the effects of treatment with vitamin C (Blackstone et al., 2004a; Blackstone et al., 2005), suggest that a similar process or processes is occurring with all three treatments. For simplicity, subsequent characterization of stolon regression thus focused on treatment with H_2O_2. To determine the extent of cell death in stolon regression, several standard assays were carried out (Costa-Pereira and Cotter, 1999; Frey, 1995; van Engeland et al., 1999; Wilson and Potten, 1999). The assays and kits used were chosen specifically for their ability to distinguish between live cells, necrotic cells and apoptotic cells. The Live–Dead Cell Staining Kit (BioVision Research Products, Mountainview, California, USA) was used on H_2O_2-treated and control colonies following the manufacturer's protocol except that seawater was substituted for staining buffer and incubation was at 20.5°C instead of 37°C. To detect phosphatidylserine, which is exposed during cell death, Annexin V-FITC Apoptosis Detection Kit (BioVision Research Products, Mountainview, CA, USA) was used on control colonies as well as colonies treated with H_2O_2. Finally, the loss of mitochondrial transmembrane potential is a characteristic of some forms of cell death. Mitochondrial membrane potential can be indicated by the cationic dye 5,5′,6,6′-tetrachloro-1,1′,3,3′-tetraethylbenzimidazolylcarbocyanine iodide. None of these *in vivo* assays produced reliable results for the stolon system of colonial hydroids. Other assays (e.g. DNA laddering) were deemed inappropriate because they are not localizable to stolon tips.

For comparisons of DNA fragmentation, the TUNEL (terminal deoxynucleotide transferase-mediated dUTP-biotin nick-end labeling) detection kit, ApoDIRECT *In Situ* DNA Fragmentation Assay Kit (BioVision Research Products, Mountainview, CA, USA), was used (van Engeland et al., 1999; Wilson and Potten, 1999). After incubation of colonies in H_2O_2, treatment solutions were replaced with plain seawater and colonies were incubated for an additional ~60 min to mimic methods used for assaying ROS and RNS. Colonies (treated and controls) were then fixed and stained following the ApoDIRECT Assay protocol with slight modifications for adherent cells. Washing steps were performed in Petri dishes using 50 ml of wash buffer for each washing step. After the staining solution was prepared, the colonies were transferred to dry Petri dishes and the staining solution was pipetted onto the colonies. Rinsing steps were performed in Petri dishes using 50 ml of rinse buffer for each rinsing step. Following rinsing, the colonies were placed in 25 ml of propidium iodide (PI)/RNase staining buffer. Fragmented DNA was labeled using terminal deoxynucleotidyl transferase to catalyze the incorporation of fluorescein-12-dUTP at the free 3′-hydroxyl ends of the DNA. The stolon cells containing fragmented DNA were visualized using fluorescence microscopy (excitation 450–490 nm, emission 515–565 nm). All stolon cells (regardless of whether or not they contained fragmented DNA) were counterstained using the PI/RNase solution and were visualized using fluorescence microscopy (excitation 546 nm, emission >590 nm). Images were obtained, measured and analyzed as described above.

Comparisons of stolon tip structure

Stolons of control colonies and colonies treated with H_2O_2 were examined using transmission electron microscopy (TEM). Following an ~60 min treatment and a subsequent ~60 min incubation in plain seawater, colonies were fixed in 2.5% glutaraldehyde for 3 h at 4°C followed by three 10 min rinses in Millonig's phosphate buffer. Specimens were postfixed in 1% osmium tetroxide for 2 h at room temperature followed by three 10 min rinses in Millonig's phosphate buffer, then dehydrated in an ethanol series and cleared in acetone. Colonies were infiltrated and embedded in EMbed 812 resin (Electron Microscopy Sciences, Hatfield, PA, USA) and sectioned on a Reichert OmU2 ultramicrotome using a diatome diamond knife. Sections of approximately 90 nm in thickness were collected on formvar-coated slot grids or 75-mesh copper grids. Sections were stained with uranyl acetate for 20 min and with lead citrate for 40 min. Subsequently, sections were examined using a Hitachi H-600 transmission electron microscope. Micrographs of specimens were obtained using Kodak 4489 electron microscope film and negatives were then scanned.

Comparisons of gastrovascular flow

Videos of stolons lasting 10 min were taken at a point ~250 μm behind the tip of a stolon using the Axiovert microscope and a Dage MTI-72 camera. Three stolon tips per colony were videotaped. A total of five H_2O_2-treated colonies and five control colonies were treated ~30 min after feeding for ~60 min and were imaged in plain seawater 90–180 min after feeding and 10–100 min after treatment. Using Image-Pro Plus, 100 images were extracted from each video at 5 s intervals. Stolon width (perisarc to perisarc) and lumen width (endoderm to endoderm) were measured for each image. Measurements of maximum and minimum lumen width were obtained for three consecutive cycles. The period (in s) of each cycle was also measured. The rate of gastrovascular flow can be estimated as lumen width (maximum – minimum) divided by cycle period and stolon width (Blackstone, 1996). Although the two-dimensional analysis of flow requires certain assumptions (e.g. Bagatto and Burggren, 2006), these assumptions seemed justifiable in this experiment.

Temporal sequence of stolon regression

To provide a better understanding of the temporal sequence of events during stolon regression, two sets of observations were carried out. First, an entire colony was treated with H_2O_2 for 1 h and observed using a dissecting microscope during and after treatment for >72 h. Second, eight stolon tips from eight different colonies were observed. Each colony was placed into a seawater-containing chamber for the Zeiss inverted microscope and videotaped prior to treatment for 5 min. H_2O_2 was then added to the chamber to a concentration of 5 mmol l^{-1}. Colonies were continually taped until regression appeared to stop, which took anywhere from 30 to 90 min. Using Image-Pro Plus, images were extracted from each video at 30 s intervals. This time-lapse sequence was then examined and the timing of events associated with stolon regression was noted.

RESULTS

Measurement of reactive oxygen species and reactive nitrogen species

As found previously with vitamin C (Blackstone et al., 2004a; Blackstone et al., 2005), treatments with H_2O_2 and NO donors typically cause regression of peripheral stolons in *P. carnea* colonies as well as a flux of ROS and RNS (Figs 2, 3). Of 63 stolons measured from control colonies in the peroxide experiments, only one exhibited regression. Of 63 stolons measured from treated colonies in the peroxide experiments, 62 exhibited regression (comparing treated to controls, χ^2=118, d.f.=1, $P \ll 0.001$). At the treatment concentration (0.5 mmol l^{-1}), fewer stolons regressed in the SNAP-treated colonies (28 out of 60), but still significantly more than the controls (3 out of 60; χ^2=27, d.f.=1, $P \ll 0.001$). When treated with either peroxide or SNAP (and whether visibly regressing or not), stolon tips exhibited high levels of endogenous peroxide-related fluorescence (Fig. 2, Fig. 4A,B). Those treated with exogenous H_2O_2 showed increased levels of ROS in stolon tips as compared to controls (Fig. 4A; F=91.4, d.f.=1, 12, $P \ll 0.001$). Those treated with exogenous SNAP also showed increased levels of ROS in stolon tips as compared to controls (Fig. 4B; F=14, d.f.=1, 12, P<0.01). When treated with either peroxide or SNAP, stolon tips exhibited high levels of endogenous NO-related fluorescence (Fig. 3, Fig. 4C,D). Those treated with exogenous H_2O_2 showed increased levels of NO in stolon tips as compared to controls (Fig. 4C; F=22.3, d.f.=1, 12, P<0.001). Those treated with exogenous SNAP also showed increased levels of NO in stolon tips as compared to controls (Fig. 4D; F=49.5, d.f.=1, 10, $P \ll 0.001$). Note that in each experiment the probe for quantifying NO or ROS must enter a cell (and have acetate groups removed) before interacting with the target molecule and exhibiting fluorescence. Thus, although there does seem to be a pattern of higher fluorescence in the treatment that is also being detected, the probes are not simply reacting with the exogenous treatment. Given these results, the process of stolon regression appears to involve increased levels of both NO and ROS.

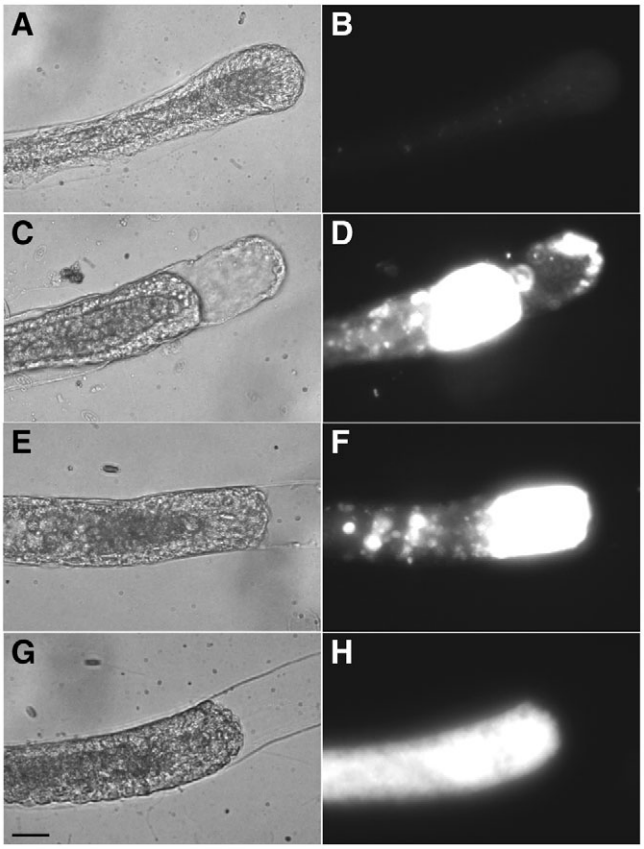

Fig. 2. Bright-field and fluorescent micrographs of stolon tips from colonies of *P. carnea*. (A,B) A healthy stolon tip (A) from a control colony exhibits relatively little peroxide-related fluorescence (B). (C,D) A regressing stolon tip (C) from a control colony exhibits an elevated level of peroxide-related fluorescence (D). (E,F) A regressing stolon tip (E) after 60 min treatment with 5 mmol l^{-1} H_2O_2 (F) exhibits an elevated level of peroxide-related fluorescence. (G,H) A regressing stolon tip (G) after 60 min treatment with 0.5 mmol l^{-1} of SNAP (H) exhibits an elevated level of peroxide-related fluorescence. Scale bar, 25 μm.

Fig. 3. Bright-field and fluorescent micrographs of stolon tips from colonies of *P. carnea*. (A,B) A healthy stolon tip (A) from a control colony exhibits relatively little NO-related fluorescence (B). (C,D) A regressing stolon tip (C) after 60 min treatment with 5 mmol l^{-1} H_2O_2 (D) exhibits an elevated level of NO-related fluorescence. (E,F) A regressing stolon tip (E) after 60 min treatment with 0.5 mmol l^{-1} SNAP (F) exhibits an elevated level of NO-related fluorescence. Scale bar, 25 μm.

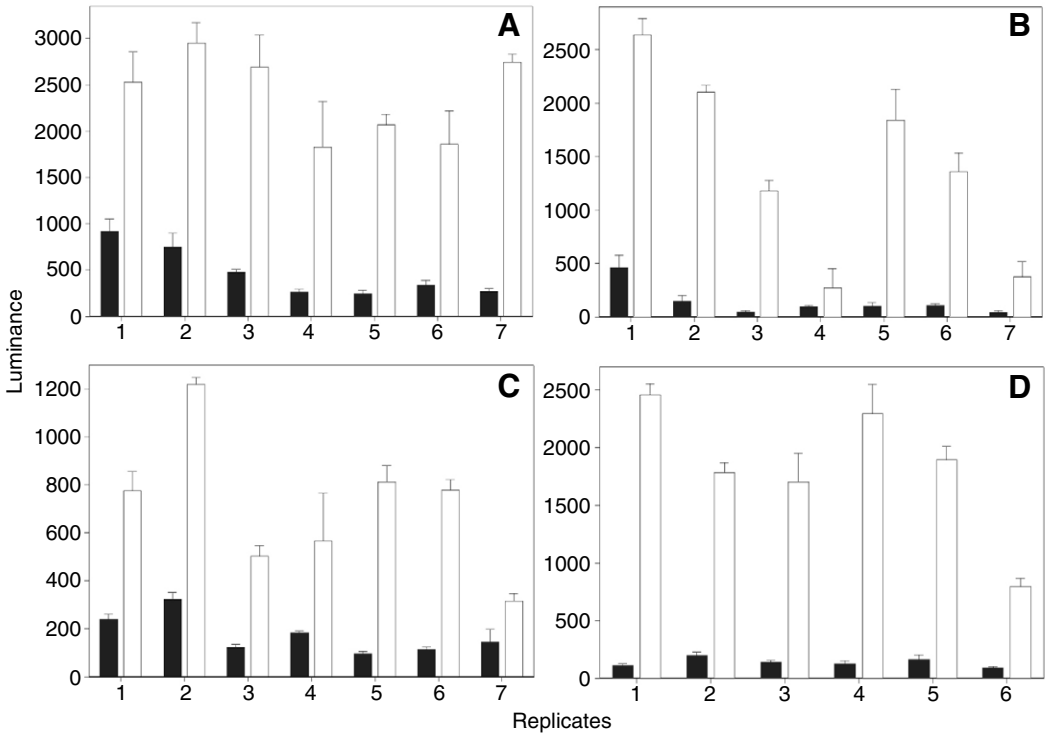

Fig. 4. Treatment with H_2O_2 or SNAP leads to an increase in ROS- and RNS-related emissions. There is an increase in (A) ROS emissions from peroxide-treated stolon tips, (B) ROS emissions from SNAP-treated stolon tips, (C) RNS emissions from peroxide-treated stolon tips, and (D) RNS emissions from SNAP-treated stolon tips. Each graph shows mean ± s.e.m. luminance (grayscale from 0 to 4095) for three stolon tips per replicate colony (filled bars, control; unfilled bars, treatment).

Cell death analyses

Regressive processes in development frequently involve cell death. Many of the standard *in vivo* assays for cell death (Costa-Pereira and Cotter, 1999; Frey, 1995; van Engeland et al., 1999; Wilson and Potten, 1999) do not work well in the hydroid stolon system and yield variable and unreliable staining (data not shown). It is probable that the molecules involved in these assays do not reliably enter an intact stolon. To detect patterns of DNA fragmentation, TUNEL assays (in which stolons are fixed and permeabilized) did show a reliable pattern of staining (Fig. 5). In H_2O_2-treated colonies, the TUNEL fluorescent images showed a strong between-treatment difference (Fig. 6A; F=119, d.f.=1, 12, $P \ll 0.001$), whereas the PI fluorescent images showed no difference between treatments (Fig. 6B; F=0.3, d.f.=1, 12, $P>0.55$). This suggests that there was no difference between treated and control stolons in the total number of cells (Fig. 5B,E), but at the same time there were many more cells with fragmented DNA in the treated stolons (Fig. 5C,F). In other studies, features of regulated cell death (e.g. DNA fragmentation, morphological changes, caspase activity) have been detected over a similar time course (Matsura et al., 2002; Blanco

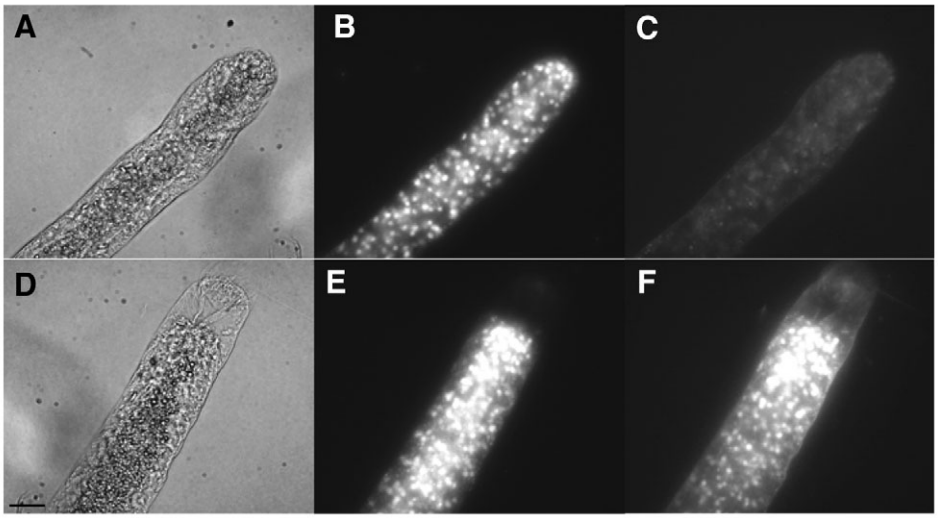

Fig. 5. Bright-field and fluorescent micrographs of stolon tips from colonies of *P. carnea*. (A–C) A healthy stolon tip (A) from a control colony has numerous cells as visualized by propidium iodide (PI) staining (B), but only a few of these cells exhibit DNA fragmentation as visualized by TUNEL staining (C). (D–F) A regressing stolon tip that was treated for 60 min with 5 mmol l^{-1} H_2O_2 (D) also has numerous cells as visualized by PI staining (E), and the majority of these cells exhibit DNA fragmentation as visualized by TUNEL staining (F). Note that the tip of the stolon has regressed in D, E and F, thus, there is no fluorescence in this area in E and F. Scale bar, 25 μm.

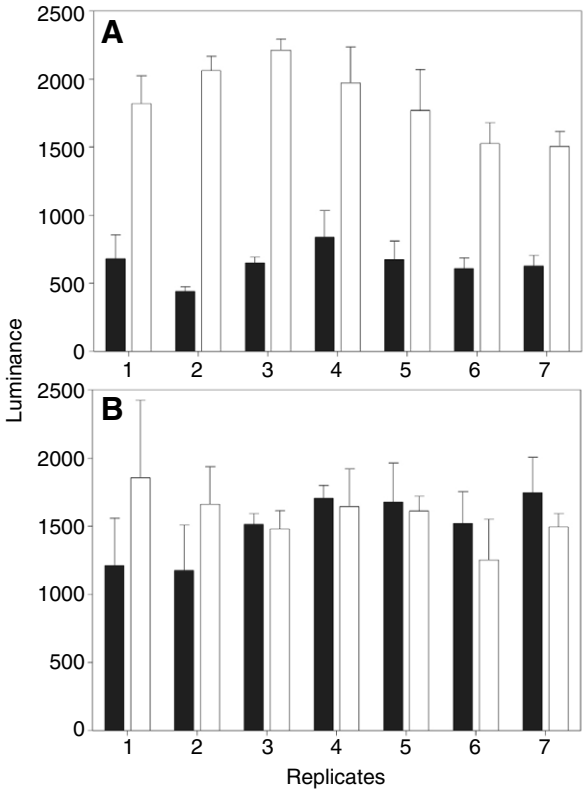

Fig. 6. Treatment with H_2O_2 leads to an increase in DNA fragmentation in the cells of stolon tips. (A) There is an increase in DNA fragmentation in cells of peroxide-treated stolon tips. Mean ± s.e.m. luminance (grayscale from 0 to 4095) of FITC-labeled dUTP for three stolon tips per replicate colony (filled bars, control; unfilled bars, 5 mmol l^{-1} H_2O_2). (B) There is no significant difference between treatments in cells labeled with PI in stolon tips. Mean ± s.e.m. luminance (grayscale from 0 to 4095) of PI-labeled cells for three stolon tips per replicate colony (filled bars, control; unfilled bars, 5 mmol l^{-1} H_2O_2).

et al., 2005; Mourdjeva et al., 2005). Note that some assays (e.g. DNA laddering) were deemed inappropriate because they cannot be restricted to stolon tips.

Comparisons of stolon tip structure

Ultrastructural features of healthy hydroid epitheliomuscular cells (EMCs) include a general columnar shape with one or more large vacuoles often surrounding the nucleus (Thomas and Edwards, 1991). Myoid processes, the contractile basal extensions of EMCs, are typically undetectable in stolon EMCs (Schierwater et al., 1992). Control and H_2O_2-treated stolons showed clear ultrastructural differences when visualized with TEM (Figs 7, 8). EMCs in control stolons had the characteristic columnar shape, typically with the cell nucleus suspended in a large vacuole (Fig. 7A–D) (Blackstone et al., 2004b), whereas the stolon tip maintained a smooth, rounded appearance (Fig. 7E). Treated stolons were often contracted (as indicated by the space between the ectoderm and the perisarc) and the cells showed extensive damage (Fig. 8A–E). The differences between cells of treated and control stolons cannot be explained entirely by contraction state of the stolon (e.g. the amount of stolon contraction in Fig. 7D and Fig. 8A appears approximately similar, but the cells look very different). Images show some recognizable features of cell death. Some of these features are characteristic of necrosis, such as flocculent condensation of chromatin (Fig. 8A,B) and vacuolation of the cytoplasm (Fig. 8A–E) (Syntichaki and Tavernarakis, 2003). Other features seem to be more characteristic of apoptosis, such as the lack of modification to cytoplasmic organelles such as mitochondria (Fig. 8C) (Syntichaki and Tavernarakis, 2003; Galluzzi et al., 2007). Compaction of the nucleus (Fig. 8A,B,D) and fragmentation of the plasma membrane into numerous small vesicles (Fig. 8A,E) also suggest apoptosis (Syntichaki and Tavernarakis, 2003; Galluzzi et al., 2007). Again, in other studies, features of regulated cell death (e.g. DNA fragmentation, morphological changes, caspase activity) have been detected over a similar time course (Matsura et al., 2002; Blanco et al., 2005; Mourdjeva et al., 2005). Not all of these features are found in all cells of treated stolons. However, none of these features has been found in any cells of non-regressing, control stolons. Indeed, Kroemer et al. (Kroemer et al., 2005) stress that it "must be remembered that dying in a cell population is not a synchronous but rather a stochastic process, and that at a given time, individual cells will be at different stages of the dying process." Thus, according to the recommendations of the Nomenclature Committee on Cell Death, cells of treated stolons exhibited five of the eight morphological features that define apoptosis, one of the five features that define necrosis, and none of the features used to define autophagy (Kroemer et al., 2005).

Comparisons of gastrovascular flow

Colonies treated with H_2O_2 exhibit greatly diminished gastrovascular flow (Fig. 9). Using lumen width divided by cycle period and stolon width as a proxy for flow rate, analysis of variance indicates a highly significant difference between controls and treated colonies (F=115, d.f.=1, 8, $P \ll 0.001$).

Temporal sequence of stolon regression

Along with stolon regression, other events occur during and after the treatment of a colony with H_2O_2. From whole-colony observation of a single treated colony (and cursory observation of numerous colonies), it appears that tentacles and polyps retract within 2 min of beginning the treatment. Shortly thereafter, the mouths of the polyps open and gastrovascular flow stops (within 5–15 min). Stolon regression was observed 15 min after treatment began. Some polyps were turning inside out after 20 min of treatment, but returned to normal configuration shortly thereafter. Within 1 h, the polyps were extended again while the tentacles remained retracted. After 1 h of treatment, the solution was replaced with plain seawater as part of the normal treatment protocol. Over the next 6 h, no change was detected in the colony except that the mouths of the polyps closed and more stolons regressed. All stolons had regressed within 4 h of treatment. The colony would not feed and gastrovascular flow could not be detected, despite the ability of the tentacles to stick to the shrimp and the ability of the polyps to move in response to the food source. The colony was able to feed again within 24 h following treatment. Gastrovascular flow was detected 2.5 h after feeding. Within 48 h after the initial treatment, regressed stolons had started to recover and the majority of stolons had recovered within 77 h. Notably, thinner stolon tips seem to regress before thicker stolon tips. Since thinner stolons typically receive less gastrovascular flow than thicker stolons (Dudgeon and Buss, 1996), this observation is consistent with the idea that gastrovascular flow is the proximate trigger of regression.

Close observation of stolon tips of eight colonies indicate that stolon regression follows a relatively stereotyped sequence of events. After treatment with H_2O_2, the first step of stolon regression involves the cessation of gastrovascular flow. In seven of the eight

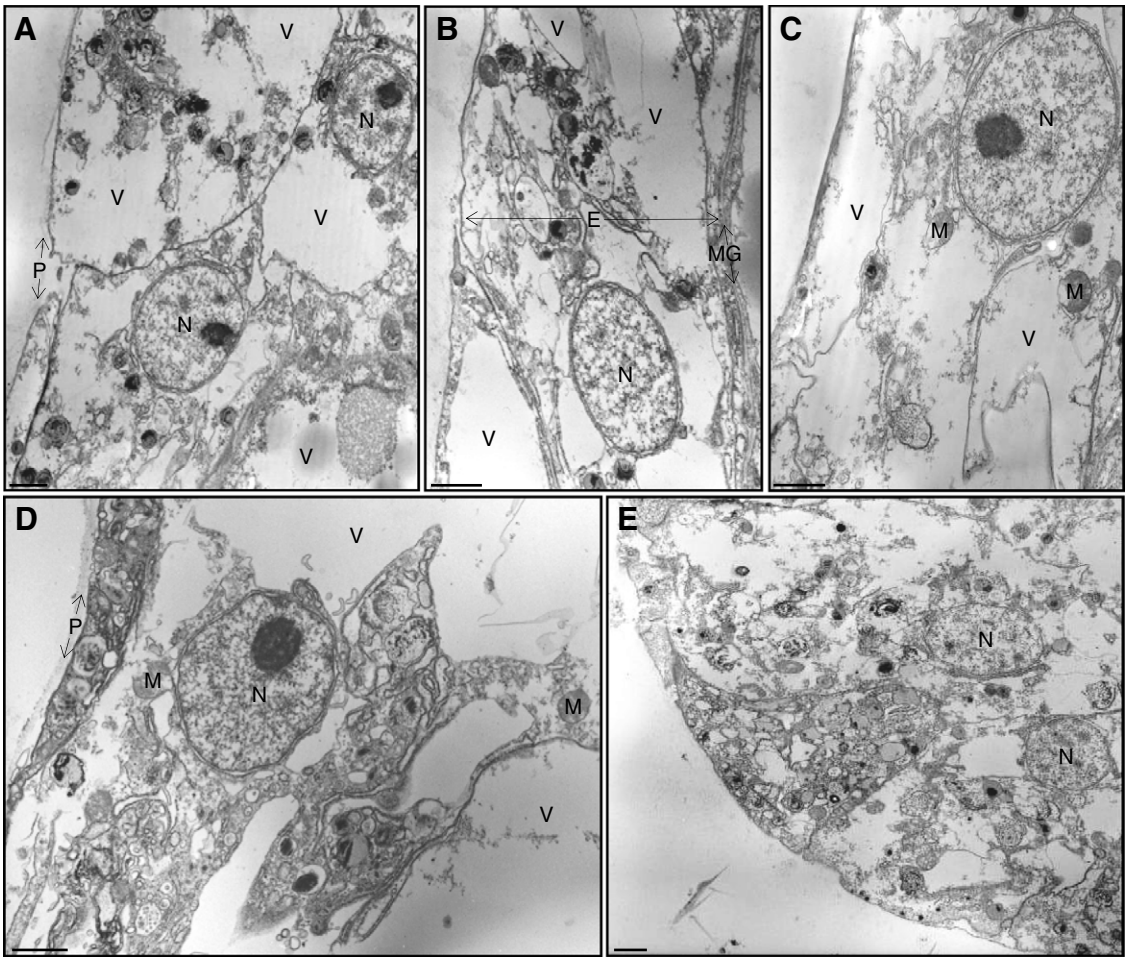

Fig. 7. TEM micrographs of a healthy stolon. (A) Epitheliomuscular cells (EMCs) in control stolons are found just inside of the perisarc and show the characteristic columnar shape. (B) The ectoderm is relatively wide (as indicated by the space between the perisarc and mesoglea) and nuclei can typically be seen suspended in a large vacuole. (C) The mitochondria of a healthy EMCs are usually about 0.5–0.75 μm. (D) Healthy EMCs near the stolon tip can be quite large as shown here. (E) The tip of a non-regressed stolon has a smooth and rounded appearance. P, perisarc; E, ectoderm; MG, mesoglea; N, nucleus; M, mitochondrion; V, vacuole. Scale bars, 1 μm.

colonies observed, this occurred within 0.5–2.0 min following treatment (13 min for the outlier). Direct observations of gastrovascular flow to tips suggest a somewhat quicker cessation of flow than whole-colony observations, possibly because (1) gastrovascular flow can be better observed at high magnification, or (2) flow to stolon tips ceases slightly before flow throughout the colony, or both. Shortly thereafter, the stolons begin to regress. In seven of the eight colonies observed, regression began 1.0–4.5 min after the initiation of treatment (49 min for the outlier). Finally, in seven of the eight colonies observed stolonal regression ceased within 8–22.5 min after treatment (90 min for the outlier). At this point, the stolon tip still appeared healthy. In some cases, regressing tips displayed a much more distorted appearance (e.g. Fig. 2G). This distortion featured a misshapen tip, often leaving small clusters of cells 'stranded' following regression (e.g. Fig. 2C). The almost immediate cessation of gastrovascular flow following treatment suggests that this event is the proximate trigger of stolon regression. Regression may thus be part of the regulation of a hydroid colony by 'self inspection' (Buss, 2001). Resolving the timing of the buildup of endogenous ROS and RNS relative to the cessation of gastrovascular flow proved difficult; for instance, the intense excitation wavelengths generated by the mercury-arc lamp of the Axiovert microscope may, by itself, affect gastrovascular flow to the stolon tip. Nevertheless, observations of numerous stolon tips (e.g. Figs 2 and 3) suggest that accumulation of endogenous ROS and RNS begins shortly after gastrovascular flow ceases.

DISCUSSION

As with many clonal organisms, colonial hydroids exhibit variation in growth form ranging from runner-like (widely spaced polyps and stolon branches) to sheet-like (closely spaced polyps and stolon branches). Rates of stolon branching relative to elongation have been thought to underlie this variation. We introduce the process of stolon regression as potentially relevant to this variation in growth form. Stolon regression occurs regularly in healthy colonies, and integrated over a long period of colony development even a modest rate of regression could potentially convert a runner-like colony into a sheet-like one. Higher rates of stolon regression may occur when colonies detect environmental signals that favor continued growth in the same location rather than outward growth. Previously, treatment with vitamin C has been shown to trigger stolon regression and sheet-like morphology (Blackstone et al., 2004a; Blackstone et al., 2005).

For detailed studies, many stolons of a colony can be reliably induced to regress by treatments with peroxide or nitric oxide. This process begins with a cessation of gastrovascular flow to the distal part of the stolon. High levels of endogenous ROS and RNS then accumulate as the stolon begins to regress. Remarkably, exogenous treatments with either H_2O_2 or a NO donor equivalently trigger endogenous formation of both H_2O_2 and NO. Transmission electron microscopy reveals that regressing stolons have atypical ultrastructural features. Cell death during regression is suggested by both TUNEL and TEM.

These results further support previous work suggesting a potentially large role for ROS and RNS in cnidarian signaling. Several examples will be briefly described to provide an appreciation of both the species and the mechanistic diversity of such signaling. First, Perez and Weis (Perez and Weis, 2006) suggest that symbiotic algae in heat-stressed anthozoans release ROS, which in turn trigger the release of NO from the host cells. By-products of this ROS–RNS signaling may contribute to anthozoan bleaching, that is, the release of the symbiotic algae. Second, Berking et al. (Berking et al., 2005) suggest that in some scyphozoans metabolically produced peroxides oxidize iodide to iodine. Endogenous tyrosine reacts with iodine to produce iodiferous tyrosine compounds. This process may trigger medusa formation, provide an oxidant defense system, and perhaps even supply the evolutionary roots of the vertebrate hormone thyroxin. Finally, building on earlier work, Doolen et al. (Doolen et al., 2007) suggest that ROS may have a crucial role in runner-like (moderate ROS) or sheet-like (low ROS) growth in *P. carnea*. The current research extends these findings by showing that, whereas moderate levels of ROS may lead to rapid colony growth and a runner-like form, high levels of ROS are involved in another process – stolon regression – which in turn may lead to more sheet-like growth. The taxonomic diversity of these results – in anthozoans, scyphozoans and hydrozoans – is matched by the diversity of pathways – host–symbiont interactions, medusa formation and colony development. The 'many pathways' view of ROS and RNS signaling in cnidarians is further supported by Blackstone et al. (Blackstone et al., 2005).

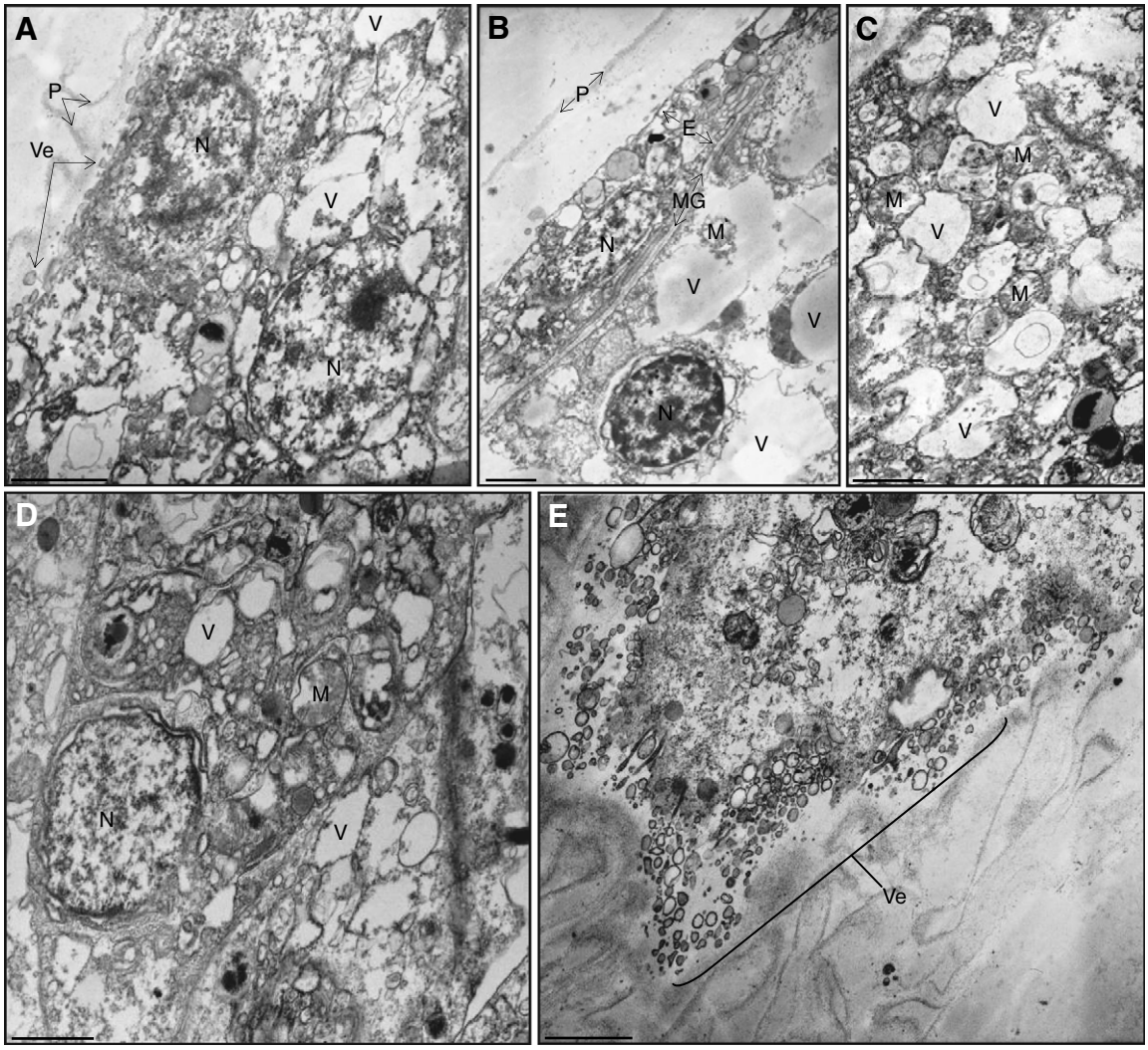

Fig. 8. TEM micrographs of a regressed stolon treated with 5 mmol l^{-1} H_2O_2. (A–C) The epitheliomuscular cells (EMCs) in a regressed stolon exhibit vacuolation of the cytoplasm (A). Treated stolons are sometimes contracted (B; as indicated by the space between the perisarc and the ectoderm). Cells of a regressed stolon have relatively normal appearing mitochondria (C) and compact nuclei with flocculent condensation of chromatin (A,B). (D,E) Cells in the tip of the regressed stolon are shrunken (D) compared to their control counterparts (e.g. Fig. 7D). Once a stolon regresses, the cell membranes in the tip form numerous small vesicles (E). P, perisarc; E, ectoderm; MG, mesoglea; N, nucleus; M, mitochondrion; V, vacuole, Ve, vesicle. Scale bars, 1 μm.

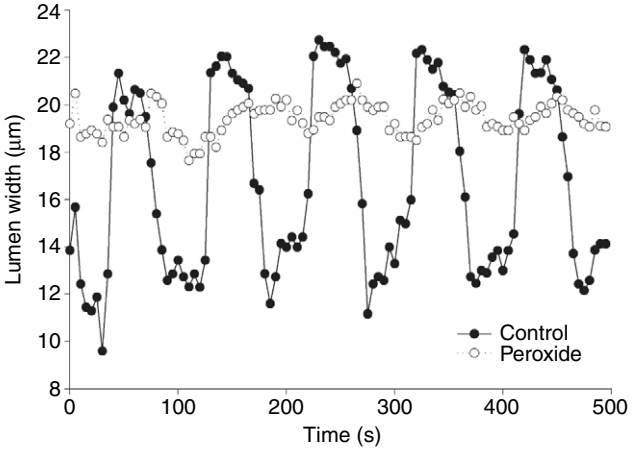

Fig. 9. Following treatment with H_2O_2, gastrovascular flow within stolon tips virtually ceases. Oscillations in lumen width (μm) over time (seconds) for stolon tips of a control colony (filled circles) and a colony treated with 5 mmol l^{-1} H_2O_2 (unfilled circles). The treated colony shows much smaller amplitudes and similar periods of oscillations; total stolon width was the same for both colonies.

Regulated cell death is increasingly accorded a prominent role in many biological processes, including those that involve tissue regression. Although programmed cell death is often equated with apoptosis, it is now clear that some forms of active or regulated cell death simply do not meet the criteria for apoptosis and that apoptosis is but one form of programmed or regulated cell death (e.g. Bredesen et al., 2006; Galluzzi et al., 2007). Thus, a plurality of cell death pathways and features is emerging (Sperandio et al., 2000; Proskuryakov et al., 2003; Syntichaki and Tavernarakis, 2003; Guimarães and Linden, 2004; Bredesen et al., 2006; Skulachev, 2006; Galluzzi et al., 2007). Regulated forms of cell death are widespread in cnidarians, and considerable work has been done to characterize these processes. In the hydrozoan *Hydra*, cell death regulates growth (David et al., 2005), disposes of nurse cells during oogenesis (Technau et al., 2003; Alexandrova et al., 2005), and eliminates allogeneic cells (Kuznetsov et al., 2002). In the hydrozoan *Hydractinia*, cell death facilitates metamorphosis (Seipp et al., 2001; Seipp et al., 2006). In anthozoans, cell death has a role in fission (Mire, 1998; Geller et al., 2005) and in bleaching (Dunn et al., 2002; Perez and Weis, 2006).

It is not clear whether or in what form cell death occurs during stolon regression. As noted in the Results, the recommendations of the Nomenclature Committee on Cell Death suggest that at least some of the features of apoptosis are found in stolon cells of treated colonies (Kroemer et al., 2005). The pulse of endogenous ROS/RNS coincident with stolon regression also suggests an active process. Certainly, other studies have documented an association between cell death pathways and ROS/RNS, both in general (e.g. Lin and Beal, 2006) and in other cnidarians (Perez and Weiss, 2006). At this point, however, conclusions that are more definitive are not possible and we would suggest that any particular form of cell death cannot be ruled in or out with the results provided. Given the constraints of the hydroid stolon system, a useful next step may be to determine the effects of inhibitors of caspases. Caspases are generally considered the effector enzymes for apoptosis (Cikala et al., 1999; Seipp et al., 2006) (but see Galluzzi et al., 2007). Investigations of this nature should provide further useful insights into the relationship between ROS/RNS, cell death and stolon regression in the development of colonial hydroids.

LIST OF ABBREVIATIONS

DAF-FM	4-amino-5-methylamino-2',7'-difluorofluorescein
DMSO	dimethyl sulfoxide
EMC	epitheliomuscular cell
H_2DCFDA	2′,7′-dichlorodihydrofluorescein diacetate
PI	propidium iodide
RNS	reactive nitrogen species
ROS	reactive oxygen species
SNAP	S-nitroso-N-acetyl-penicillamine
TEM	transmission electron microscopy
TUNEL	terminal deoxynucleotide transferase-mediated dUTP-biotin nick-end labeling

Detailed and helpful comments from two anonymous reviewers were useful in revising earlier versions of this manuscript. The National Science Foundation (IBN-00-90580 and EF-05-31654) supported this research.

REFERENCES

Alexandrova, O., Schade, M., Böttger, A. and David, C. N. (2005). Oogenesis in Hydra: nurse cells transfer cytoplasm directly to the growing oocyte. *Dev. Biol.* **281**, 91-101.

Armstrong, J. S., Whiteman, M., Yang, H. and Jones, D. P. (2004). The redox regulation of intermediary metabolism by a superoxide-aconitase rheostat. *BioEssays* **26**, 895-900.

Bagatto, B. and Burggren, W. (2006). A three-dimensional functional assessment of heart and vessel development in the larva of the zebrafish (*Danio rerio*). *Physiol. Biochem. Zool.* **79**, 194-201.

Beloussov, L. V. (1973). Growth and morphogenesis of some marine Hydrozoa according to histological data and time-lapse studies. *Publ. Seto Mar. Biol. Lab.* **20**, 315-366.

Beloussov, L. V., Labas, J. A., Kazakova, N. I. And Zaraisky, A. G. (1989). Cytophysiology of growth pulsations in hydroid polyps. *J. Exp. Zool.* **249**, 258-270.

Berking, S., Czech, N., Gerharz, M., Herrman, K., Hoffman, U., Raifer, H., Sekul, G., Siefker, B., Sommerei, A. and Vedder, F. (2005). A newly discovered oxidant defense system and its involvement in the development of *Aurelia aurita* (Scyphozoa, Cnidaria): reactive oxygen species and elemental iodine control medusa formation. *Int. J. Dev. Biol.* **49**, 969-976.

Blackstone, N. W. (1996). Gastrovascular flow and colony development in two colonial hydroids. *Biol. Bull. Mar. Biol. Lab. Woods Hole* **190**, 56-68.

Blackstone, N. W. (1997). Dose-response relationships for experimental heterochrony in a colonial hydroid. *Biol. Bull. Mar. Biol. Lab. Woods Hole* **193**, 47-61.

Blackstone, N. W. (1999). Redox control in development and evolution: evidence from colonial hydroids. *J. Exp. Biol.* **202**, 3541-3553.

Blackstone, N. W., Cherry, K. S. and Van Winkle, D. H. (2004a). The role of polyp-stolon junctions in the redox signaling of colonial hydroids. *Hydrobiologia* **530/531**, 291-298.

Blackstone, N. W., Cherry, K. S. and Glockling, S. L. (2004b). Structure and signaling in polyps of a colonial hydroid. *Invert. Biol.* **123**, 43-53.

Blackstone, N. W., Bivins, M. J., Cherry, K. S., Fletcher, R. E. and Geddes, G. C. (2005). Redox signaling in colonial hydroids: many pathways for peroxide. *J. Exp. Biol.* **208**, 383-390.

Blanco, G. A., Bustamante, J., Garcia, M. and Hajos, S. (2005). Hydrogen peroxide induces apoptotic-like cell death in coelomocytes of *Themiste petricola* (Sipuncula). *Biol. Bull.* **209**, 168-183.

Bredesen, D. E., Rao, R. V. and Mehlen, P. (2006). Cell death in the nervous system. *Nature* **443**, 796-802.

Buss, L. W. (2001). Growth by intussusception in hydractiniid hydroids. In *Evolutionary Patterns* (ed. J. B. C. Jackson, S. Lidgard and F. K. McKinney), pp. 3-26. Chicago, IL: University of Chicago Press.

Buss, L. W. and Blackstone, N. W. (1991). An experimental exploration of Waddington's epigenetic landscape. *Philos. Trans. R. Soc. Lond. B Biol. Sci.* **332**, 49-58.

Cartwright, P. and Buss, L. W. (1999). Colony integration and the expression of the *Hox* gene, *Cnox-2*, in *Hydractinia symbiolongicarpus* (Cnidaria: Hydrozoa). *J. Exp. Zool. B Mol. Dev. Evol.* **285**, 57-62.

Cartwright, P., Bowsher, J. and Buss, L. W. (1999). Expression of a Hox gene, *Cnox-2*, and the division of labor in a colonial hydroid. *Proc. Natl. Acad. Sci. USA* **96**, 2183-2186.

Cartwright, P., Schierwater, B. and Buss, L. W. (2006). Expression of a *Gsx* parahox gene, *Cnox-2*, in colony ontogeny in *Hydractinia* (Cnidaria:Hydrozoa). *J. Exp. Zool. B Mol. Dev. Evol.* **306**, 1-10.

Cikala, M., Wilm, B., Hobmayer, E., Bottger, A. and David, C. (1999). Identification of caspases and apoptosis in the simple metazoan *Hydra*. *Curr. Biol.* **9**, 959-962.

Costa-Pereira, A. P. and Cotter, T. G. (1999). Metabolic alterations associated with apoptosis. In *Apoptosis: A Practical Approach* (ed. G. Studzinski), pp. 141-156. New York: Oxford University Press.

David, C. N., Schmidt, N., Schade, M., Pauly, B., Alexandrova, O. and Böttger, A. (2005). *Hydra* and the evolution of apoptosis. *Integr. Comp. Biol.* **45**, 631-638.

Doolen, J. F., Geddes, G. C. and Blackstone, N. W. (2007). Multicellular redox regulation in an early-evolving animal treated with glutathione. *Physiol. Biochem. Zool.* **80**, 317-325.

Dudgeon, S. R. and Buss, L. W. (1996). Growing with the flow: on the maintenance and malleability of colony form in the hydroid *Hydractinia*. *Am. Nat.* **147**, 667-691.

Dunn, S. R., Bythell, J. C., Le Tissier, M. D. A., Burnett, W. J. and Thomason, J. C. (2002). Programmed cell death and cell necrosis activity during hyperthermic

stress-induced bleaching of the symbiotic sea anemone *Aiptasia* sp. *J. Exp. Mar. Biol. Ecol.* **272**, 29-53.
Filomeni, G., Rotilio, G. and Ciriolo, M. R. (2005). Disulfide relays and phosphorylation cascades: partners in redox-mediated signaling pathways. *Cell Death Differ.* **12**, 1555-1563.
Finkel, T. (2001). Reactive oxygen species and signal transduction. *IUBMB Life* **52**, 3-6.
Frey, T. (1995). Nucleic acid dyes for detection of apoptosis in live cells. *Cytometry* **21**, 265-274.
Galluzzi, L., Maiuri, M. C., Vitale, I., Zischka, H., Castedo, M., Zitvogel, L. and Kroemer, G. (2007). Cell death modalities: classification and pathophysiological implications. *Cell Death Differ.* **14**, 1237-1266.
Geller, J. B., Fitzgerald, L. J. and King, C. E. (2005). Fission in sea anemones: integrative studies of life cycle evolution. *Integr. Comp. Biol.* **45**, 615-622.
Guimarães, C. A. and Linden, R. (2004). Programmed cell death: apoptosis and alternative deathstyles. *Eur. J. Biochem.* **271**, 1638-1650.
Hale, L. J. (1964). Cell movements, cell division, and growth in the hydroid *Clytia johnstoni*. *J. Embryol. Exp. Morphol.* **12**, 517-538.
Hori, S., Kobayashi, A. and Natori, S. (2000). A novel homocyte-specific membrane protein of *Sarcophaga* (flesh fly). *Eur. J. Biochem.* **267**, 5397-5403.
Jantzen, H., Hassel, M. and Schulze, I. (1998). Hydroperoxides mediate lithium effects on regeneration in *Hydra*. *Comp. Biochem. Physiol.* **119C**, 165-175.
Kojima, H., Urano, Y., Kikuchi, K., Higuchi, M. and Hirata, K. (1999). Fluorescent indicators for imaging nitric oxide production. *Angew. Chem. Int. Ed. Engl.* **38**, 3209-3212.
Kroemer, G., El-Deiry, W. S., Golstein, P., Peter, M. E., Vaux, D., Vandenabeele, P., Zhivotovsky, B., Blagosklonny, M. V., Malorni, W., Knight, R. A. et al. (2005). Classification of cell death: recommendations of the Nomenclature Committee on Cell Death. *Cell Death Differ.* **12**, 1463-1467.
Kuznetsov, S. G., Anton-Erxleben, F. and Bosch, T. C. G. (2002). Epithelial interactions in *Hydra*: apoptosis in interspecies grafts is induced by detachment from the extracellular matrix. *J. Exp. Biol.* **205**, 3809-3817.
Lange, R. G. and Müller, W. A. (1991). SIF, a novel morphogenetic inducer in Hydrozoa. *Dev. Biol.* **147**, 121-132.
Lee, J.-W. and Helmann, J. D. (2006). The PerR transcription factor senses H_2O_2 by metal-catalysed histidine oxidation. *Nature* **440**, 363-367.
Lin, M. T. and Beal, M. F. (2006). Mitochondrial dysfunction and oxidative stress in neurodegenerative diseases. *Nature* **443**, 787-795.
Lohmann, I., McGinnis, N., Bodmer, M. and McGinnis, W. (2002). The *Drosophila Hox* gene *Deformed* sculpts head morphology via direct regulation of the apoptosis activator *reaper*. *Cell* **110**, 457-466.
Matsura, T., Serinkan, B. F., Jiang, J. and Kagan, V. E. (2002). Phosphatidylserine peroxidation/externalization during staurosporine-induced apoptosis in HL-60 cells. *FEBS Lett.* **524**, 25-30.
Mire, P. (1998). Evidence for stretch-regulation of fission in a sea anemone. *J. Exp. Zool.* **282**, 344-359.
Mourdjeva, M., Kyurkchiev, D., Mandinova, A., Altankova, I., Kehayov, I. and Kyurkchiev, S. (2005). Dynamics of membrane translocation of phosphatidylserine during apoptosis detected by a monoclonal antibody. *Apoptosis* **10**, 209-217.
Perez, S. and Weis, V. (2006). Nitric oxide and cnidarian bleaching: an eviction notice mediates breakdown of a symbiosis. *J. Exp. Biol.* **209**, 2804-2810.
Plickert, G., Heringer, A. and Hiller, B. (1987). Analysis of spacing in a periodic pattern. *Dev. Biol.* **120**, 399-411.
Ponczek, L. M. and Blackstone, N. W. (2001). Effects of cloning rate on fitness-related traits in two marine hydroids. *Biol. Bull. Mar. Biol. Lab. Woods Hole* **201**, 76-83.
Proskuryakov, S. Y., Konoplyannikov, A. G. and Gabai, V. L. (2003). Necrosis: a specific form of programmed cell death? *Exp. Cell Res.* **283**, 1-16.
Salmeen, A., Andersen, J. N., Meyers, M. P., Meng, T.-C., Hinks, J. A., Tonks, N. K. and Barford, D. (2003). Redox regulation of protein tyrosine phosphatase 1B involves a suphenyl-amide intermediate. *Nature* **423**, 769-773.
Schaller, H. C., Hoffmeister, S. A. and Dübel, S. (1989). Role of the neuropeptide head activator for growth and development in hydra and mammals. *Dev. Suppl.* **1999**, 99-107.
Schierwater, B., Piekos, B. and Buss, L. W. (1992). Hydroid stolonal contractions mediated by contractile vacuoles. *J. Exp. Biol.* **162**, 1-21.
Seipp, S., Schmich, J. and Leitz, T. (2001). Apoptosis – a death-inducing mechanism tightly linked with morphogenesis in *Hydractinia echinata* (Cnidaria, Hydrozoa). *Development* **128**, 4891-4898.
Seipp, S., Wittig, K., Stiening, B., Böttger, A. and Leitz, T. (2006). Metamorphosis of *Hydractinia echinata* (Cnidaria) is caspase-dependent. *Int. J. Dev. Biol.* **50**, 63-70.
Skulachev, V. P. (2006). Bioenergetic aspects of apoptosis, necrosis, and mitoptosis. *Apoptosis* **11**, 473-485.
Sperandio, S., de Belle, I. and Bredesen, D. E. (2000). An alternative, nonapoptotic form of programmed cell death. *Proc. Natl. Acad. Sci. USA* **97**, 14376-14381.
Syntichaki, P. and Tavernarakis, N. (2003). The biochemistry of neuronal necrosis: rogue biology? *Nat. Rev. Neurosci.* **4**, 672-684.
Takahashi, T., Muneoka, Y., Lohman, J., Lopez de Haro, M. S., Solleder, G., Bosch, T. C. G., David, C. N., Bode, H. R., Koizumi, O., Shimizu, H. et al. (1997). Systematic isolation of peptide signal molecules regulating development in hydra: LWamide and PW families. *Proc. Natl. Acad. Sci. USA* **94**, 1241-1246.
Tata, J. R. (2006). Amphibian metamorphosis as a model for the developmental actions of thyroid hormone. *Mol. Cell. Endocrinol.* **246**, 10-20.
Technau, U., Miller, M. A., Bridge, D. and Steele, R. E. (2003). Arrested apoptosis of nurse cells during Hydra oogenesis and embryogenesis. *Dev. Biol.* **260**, 191-206.
Thomas, M. B. and Edwards, N. C. (1991). Cnidaria: Hydrozoa. In *Microscopic Anatomy of Invertebrates*. Vol. 2 (ed. F. W. Harrison and J. A. Westfall), pp. 91-183. New York: Wiley-Liss.
van Engeland, M., Schutte, B., Hopman, A. H. N., Ramaekers, F. C. S. and Reutelingsperger, C. P. M. (1999). Cytochemical detection of cytoskeletal and nucleoskeletal changes during apoptosis. In *Apoptosis: A Practical Approach* (ed. G. Studzinski), pp. 125-140. New York: Oxford University Press.
van Kleunen, M. and Fisher, M. (2001). Adaptive evolution of plastic foraging responses in a clonal plant. *Ecology* **82**, 3309-3319.
van Montfort, R. L. M., Congreve, M., Tisi, D., Carr, R. and Jhoti, H. (2003). Oxidation state of the active-site cysteine in protein tyrosine phosphatase 1B. *Nature* **423**, 773-777.
Vernole, P., Tedeschi, B., Caporossi, D., Maccarrone, M., Melino, G. and Annicchiarico-Petruzzelli, M. (1998). Induction of apoptosis by bleomycin in resting and cycling human lymphocytes. *Mutagenesis* **13**, 209-215.
Wilson, J. W. and Potten, C. S. (1999). Morphological recognition of apoptotic cells. In *Apoptosis: A Practical Approach* (ed. G. Studzinski), pp. 19-39. New York: Oxford University Press.
Wyttenbach, C. R. (1968). The dynamics of stolon elongation in the hydroid, *Campanularia flexuosa*. *J. Exp. Zool.* **167**, 333-352.
Wyttenbach, C. R. (1969). Genetic variations in the mode of stolon growth in the hydroid, *Campanularia flexuosa*. *Biol. Bull.* **137**, 547-556.
Wyttenbach, C. R. (1973). The role of hydroplasmic pressure in stolon growth movements in the hydroid, *Bougainvillia*. *J. Exp. Zool.* **186**, 79-90.
Zuzarte-Luís, V. and Hurlé, J. M. (2002). Programmed cell death in the developing limb. *Int. J. Dev. Biol.* **46**, 871-876.